

Short Communication

Study of Tetraethylammonium bis(trifluoromethylsulfonyl)imide as a Supporting Electrolyte for an All-organic Redox Flow Battery Using Benzophenone and 1,4-di-tert-butyl-2,5-dimethoxybenzene as Active Species

Xiang Wang^{1,2}, Xueqi Xing^{1,2}, Yongjie Huo^{1,2}, Yicheng Zhao^{1,2}, Yongdan Li^{1,2,3}, Hong Chen^{4,*}

¹ State Key Laboratory of Chemical Engineering (Tianjin University), Tianjin Key Laboratory of Applied Catalysis Science and Technology, School of Chemical Engineering, Tianjin University, Tianjin 300072, China

² Collaborative Innovation Center of Chemical Science and Engineering (Tianjin), Tianjin, 300072, China.

³ Department of Chemical and Metallurgical Engineering, School of Chemical Engineering, Aalto University, Kemistintie 1, FI-00076 Aalto, Finland

⁴ School of Environmental Science and Engineering, Tianjin University, Tianjin 300072, China

*E-mail: chenhong_0405@tju.edu.cn

Received: 12 March 2018 / Accepted: 8 May 2018 / Published: 5 June 2018

An ionic liquid tetraethylammonium bis(trifluoromethylsulfonyl)imide (TEATFSI) is synthesized as the supporting electrolyte in an all-organic redox flow battery system with acetonitrile as the solvent. Benzophenone (BP) and 1,4-di-tert-butyl-2,5-dimethoxybenzene (DBB) are used as the redox active species. The battery exhibits a high open voltage of 2.95 V. The electrode reactions are controlled by diffusion, which is significantly influenced by the cations of the supporting electrolytes. With TEATFSI as the supporting electrolyte, the diffusion coefficients are $1.21\text{-}1.43\times 10^{-5}\text{ cm}^2\text{ s}^{-1}$ and $0.89\text{-}1.16\times 10^{-5}\text{ cm}^2\text{ s}^{-1}$ at anode and cathode, respectively. The coulombic, voltage and energy efficiencies of the battery are 97%, 46% and 44%, respectively. The battery shows a stable performance during 50 charge-discharge cycles.

Keywords: All organic redox flow battery, Ionic liquid, Energy storage, Supporting electrolyte, Tetraethylammonium bis(trifluoromethylsulfonyl)imide

1. INTRODUCTION

The utilization of renewable energy sources such as solar, wind, ocean and geothermal energy as sustainable and environmental friendly alternatives to fossil fuels has been developed rapidly in

recent years [1]. Owing to the features of output fluctuation and unpredictability of the renewable energy sources, electrical energy storage systems are highly required to improve the reliability and availability of the power systems [2]. As a large-scale energy storage technology, redox flow batteries (RFBs) are promising load leveling devices [3]. Many RFBs based on aqueous chemistries have been designed and developed for commercial applications such as all-vanadium RFBs [4, 5] and zinc-bromine RFBs [6, 7]. Compared with these aqueous RFBs, non-aqueous RFBs (NARFBs) utilizing organic solvents in electrolytes offer a wide working temperature range, a wide electrochemical stability window (ESW) and high solubility for most organic redox active species, which makes them able to offer high cell voltage and energy density by optimizing the components of electrolytes [8].

NARFBs using organic active materials and solvents in electrolytes are referred to as all-organic RFBs. Ideal redox active materials for all-organic RFBs should have a redox potential near the upper or lower edge of the ESW of the electrolyte, high solubility and stability [9]. 1,4-di-tert-butyl-2,5-dimethoxybenzene (DBB) is an excellent redox shuttle additive for overcharge protection of lithium-ion batteries, which is able to support over 300 cycles (100% overcharged) and shows a high half-wave potential of 4.32 V (vs. Li/Li⁺) [10]. Recently, a number of 1,4-dimethoxybenzene derivatives have been studied as the cathode active materials to provide a high cathode potential for lithium-ion redox flow batteries [11, 12]. However, NARFB using DBB as the catholyte has been rarely studied. As for the anode active species, benzophenone (BP) is considered as a suitable anolyte of NARFB due to its low redox potential and high electrochemical reversibility [13]. Nevertheless, the stability of the battery requires further improvement [14, 15].

In general, the ionic conductivities of pure organic solvents are quite low, which could be improved by the addition of supporting electrolytes [8]. Until now, most of the supporting electrolytes have been studied in non-aqueous vanadium RFBs are ionic liquids due to their high conductivity, wide ESW and high stability [16]. Tetrafluoroborate (BF₄⁻), hexafluorophosphate (PF₆⁻) and bis(trifluoromethanesulfonyl)imide (TFSI⁻) are promising anions used in NARFB for their advantages such as low toxicity, easy preparation, good chemical stability and thermal stability [17]. Among the common non-reactive cations, quaternary ammonium, such as tetraethylammonium (TEA⁺) and tetrabutylammonium (TBA⁺), and imidazolium, such as 1-ethyl-3-methylimidazolium (EMIM⁺), are used to compose ionic liquids for non-aqueous electrochemistry because they are electrochemically stable over an appropriate voltage window [16, 18, 19]. Ionic liquids such as TEABF₄ and TEAPF₆ have been widely used as the supporting electrolytes of NARFBs [20, 21]. However, possible reactions between the organic radical ions and BF₄⁻/PF₆⁻ may cause the degradation of the active species and the instability of the flow cell [22]. Wei [23] has studied TEATFSI as a supporting electrolyte in acetonitrile (AN) solvent. With 9-fluorenone (FL) and 2,5-di-tert-butyl-1-methoxy-4-[2'-methoxyethoxy]benzene (DBMMB) as the anode and the cathode redox materials, respectively, the NARFB exhibited a cell voltage of 2.37 V and a high durability of more than 50 stable cycles. In this work, a high potential all-organic RFB system is fabricated using BP and DBB as the anode and the cathode active species, respectively. Various ionic liquids are investigated as the supporting electrolytes. The effects of the supporting electrolyte on the performance of the all-organic RFB are studied.

2. EXPERIMENTAL

2.1. Materials and purification

Six ionic liquids were used as supporting electrolytes. TEABF₄ (99%), TEAPF₆ (99%), TBABF₄ (98%) and TBAPF₆ (99%) were purchased from 9ding Chemical (Shanghai) Co., Ltd. and dried in vacuum at 60 °C over 24 hours before use. EMIMTFSI (99%) was purchased from Adamas Reagent Co., Ltd. and used without further purification. TEATFSI was synthesized through a two-step method. Tetraethylammonium bromide was firstly prepared through the reaction between pure triethylamine (Tianjin Guangfu Fine Chemical Research Institute, China) and ethyl bromide (Tianjin Guangfu Fine Chemical Research Institute, China) at 55 °C for 24 h. After washed with tetrahydrofuran and filtered, the solid was dried in vacuum at 80 °C for 48 h. The obtained tetraethylammonium bromide and lithium bis(trifluoromethanesulphonyl)imide (Shanghai D&B biotechnology Co., Ltd., China) were dissolved in deionized water and stirred at 50 °C for 20 h to get crystallites. The product was rinsed with deionized water and dried in vacuum at 30 °C for 48 h.

The solvent AN (99%, Shanghai Macklin Biochemical Co., Ltd., China) was distilled with calcium hydride under nitrogen to remove the dissolved oxygen. The active species BP (98%, Tianjin Guangfu Fine Chemical Research Institute, China) and DBB (98%, Bide Pharmatech Ltd., China) were dried in vacuum at 30 °C over 12 h prior to use.

2.2. Electrochemical measurements

The conductivity of the AN solution containing 0.1 mol L⁻¹ TEATFSI without active species was measured using a conductivity meter (DDS-307A, REX, INESA Scientific Instrument Co., Ltd., China) at 25 °C. Cyclic voltammetry (CV) measurements were carried out with an electrochemical workstation (VersaSTAT 3, Princeton Applied Research, USA) at 25 °C. A three-electrode system was fabricated. The working electrode was a glassy-carbon electrode with a diameter of 6 mm (Aidahengsheng, China). The reference electrode was an Ag/Ag⁺ electrode (0.5 mol L⁻¹ AgNO₃ in AN, Aidahengsheng, China). The counter electrode was a graphite plate with a geometry surface area of 5.24 cm². The electrolyte, which contained 0.01 mol L⁻¹ BP, 0.01 mol L⁻¹ DBB and 0.1 mol L⁻¹ supporting electrolyte in AN was deoxygenated with nitrogen (≥99.999%, Liufang, China) for about 15 min prior to all the experiments. The CV curves were recorded in the potential range from -2.5 to 1.1 V (vs. Ag/Ag⁺) at scan rates ranging from 0.07 to 0.6 V s⁻¹.

The diffusion coefficients of the redox species in the electrolytes were estimated based on the Randlese-Sevcik equation. For a reversible electron transfer reaction:

$$i_p = 2.69 \times 10^5 n^{3/2} A c D^{1/2} \nu^{1/2} \quad (1)$$

For an irreversible electron transfer reaction:

$$i_p = 2.99 \times 10^5 n^{3/2} \alpha^{1/2} A c D^{1/2} \nu^{1/2} \quad (2)$$

In the equations, i_p is the peak current (A), n the number of electrons transferred in the redox reaction process ($n = 1$), α the transfer coefficient ($\alpha = 0.5$), A the electrode area (cm²), c the primary

redox species concentration (mol L^{-1}), ν the scan rate (V s^{-1}) and D the diffusion coefficient ($\text{cm}^2 \text{s}^{-1}$). All the experiments were performed three times for checking the repeatability at room temperature.

2.3. Flow cell tests

The cyclic charge-discharge experiments were performed with the electrochemical workstation using an in-house-designed flow battery system placed in an Ar-filled glove box at room temperature. A polyethylene-based microporous separator (175 μm thick, 58% porosity, 0.1-1 μm pore size, Daramic, USA) was used as the separator between two graphite felt electrodes (20 mm \times 20 mm \times 5 mm, Hunan Jiuhua Carbon Hi-Tech Co., Ltd., China). Both graphite felts had a compression ratio of about 10% to ensure optimal electrical conductivity.

The volumes of the positive electrolyte and the negative electrolyte were both 10 mL. Both electrolytes were circulated through the cell with two peristaltic pumps (BT100-1L, Longer Precision Pump Co., Ltd., China) at a flow rate of 50 mL min^{-1} . The concentrations of the supporting electrolyte and active species were the same as those in the CV tests. Cyclic charge-discharge tests were conducted between 3.2 V and 1.0 V at a constant current density of 1.0 mA cm^{-2} .

3. RESULTS AND DISCUSSION

3.1. Electrochemical measurements

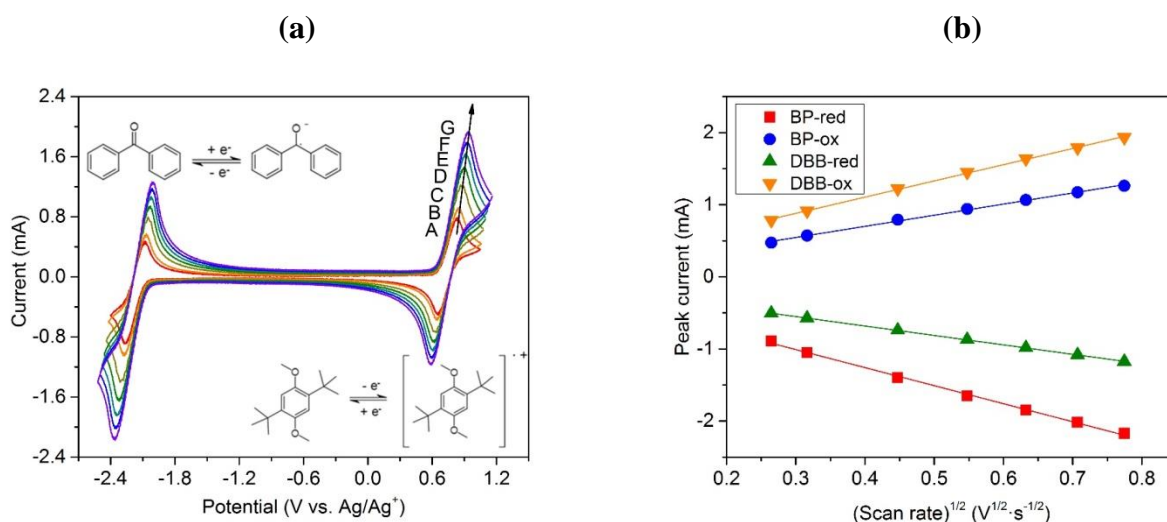


Figure 1. (a) Cyclic voltammogram of 0.01 mol L^{-1} BP and 0.01 mol L^{-1} DBB in 0.1 mol L^{-1} TEATFSI/AN with different scanning rates: (A) 0.07 V s^{-1} , (B) 0.1 V s^{-1} , (C) 0.2 V s^{-1} , (D) 0.3 V s^{-1} , (E) 0.4 V s^{-1} , (F) 0.5 V s^{-1} and (G) 0.6 V s^{-1} . (b) The relationship between the peak currents of the electrode reactions and the scanning rate.

The conductivity of the AN solution containing 0.1 mol L^{-1} TEATFSI is 4.76 mS cm^{-1} , which meets the requirement for the electrolyte [24]. In Fig. 1a, the CV curves of the battery with TEATFSI

as the supporting electrolyte show two redox couples with the centres at -2.19 V and 0.76 V vs. Ag/Ag^+ , which result in an open cell voltage of 2.95 V for the flow battery. The peak currents of all of the redox reactions are linearly related to the square root of the scanning rate (Fig. 1b), indicating that the reactions are under diffusion control. The diffusion coefficients are calculated according to Eqs. 1 and 2, which are in the range of $1.21\text{--}1.43 \times 10^{-5} \text{ cm}^2 \text{ s}^{-1}$ and $0.89\text{--}1.16 \times 10^{-5} \text{ cm}^2 \text{ s}^{-1}$ for BP and DBB, respectively.

Fig. 2 shows the ranges of diffusion coefficients of BP and DBB in AN with different supporting electrolytes. The cations of the supporting electrolytes show a significant effect on the diffusion coefficients of both BP and DBB, while the influence of the anions is much weaker. For both BP and DBB, the highest diffusion coefficients, which are above $10^{-5} \text{ cm}^2 \text{ s}^{-1}$, are obtained in the electrolytes containing TEA^+ . The diffusion coefficients are much higher than those in most of the previous works [22, 25–28]. Since the electrode reactions are controlled by diffusion, a fast diffusion process would improve the reaction kinetics. On the contrary, sluggish diffusion happens in the electrolytes with TBA^+ . Meanwhile, the diffusion of DBB is slightly slower than that of BP in all of the electrolytes.

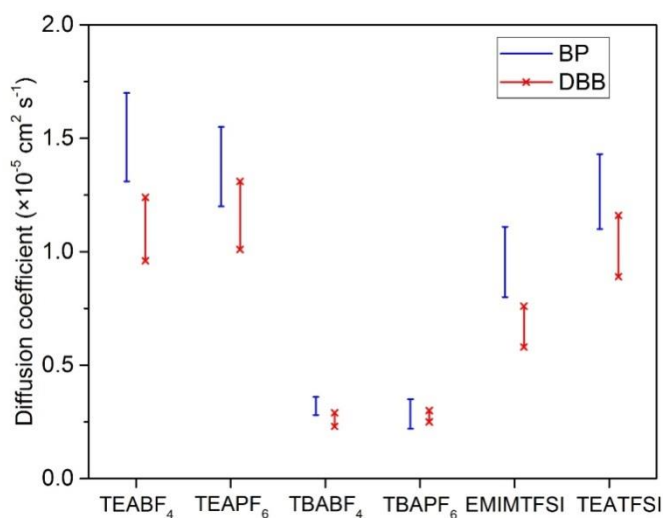


Figure 2. The diffusion coefficients of BP and DBB in AN with different supporting electrolytes.

3.2. Charge/discharge tests

Fig. 3 shows the cycling performance of the all-organic RFB with 0.1 mol L^{-1} TEATFSI as the supporting electrolyte. Only one charge plateau is observed, agreeing with the results in Fig. 1a. During the first six cycles (Fig. 3a), the charge plateau appears around $2.9\text{--}3.1$ V, while the discharge plateau is around $1.8\text{--}2.0$ V. After fifty charge-discharge cycles, the discharge plateau falls slightly to about 1.7 V.

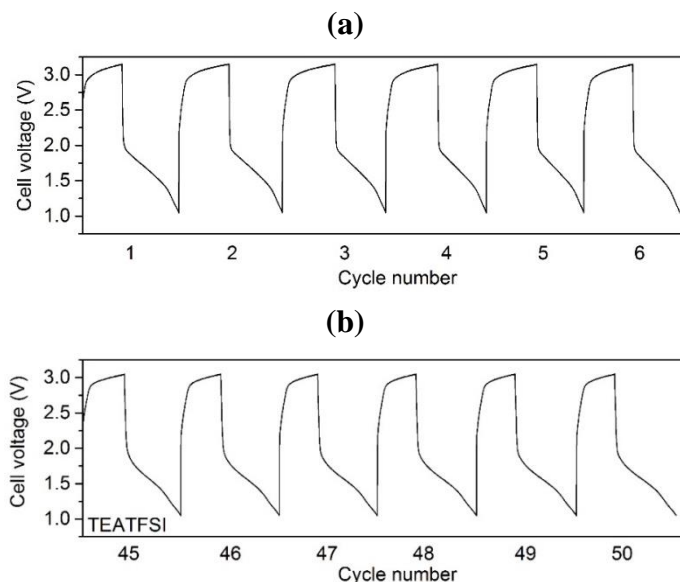


Figure 3. Cyclic charge-discharge curves of the battery with TEATFSI as the supporting electrolyte. (a) The first six cycles and (b) the last six cycles.

Fig. 4 shows the cycling efficiency and capacity of the flow battery with TEATFSI as the supporting electrolyte. During fifty charge-discharge cycles, the coulombic efficiency (CE) increases slightly from 95% to 98%, while the voltage efficiency (VE) and the energy efficiency (EE) both keep almost constant at 46% and 44%, respectively. On the contrary, the charge/discharge capacity of the battery drops quickly during the first 10 cycles with a decrease of about 11%, and then declines gradually during the next 40 cycles. During the charge/discharge circles, $BP^{\cdot-}$ and $DBB^{\cdot+}$ radical ions are formed at the anode and the cathode sides, respectively. The chemically reactive radicals would impact the cycling stability of the flow cell.

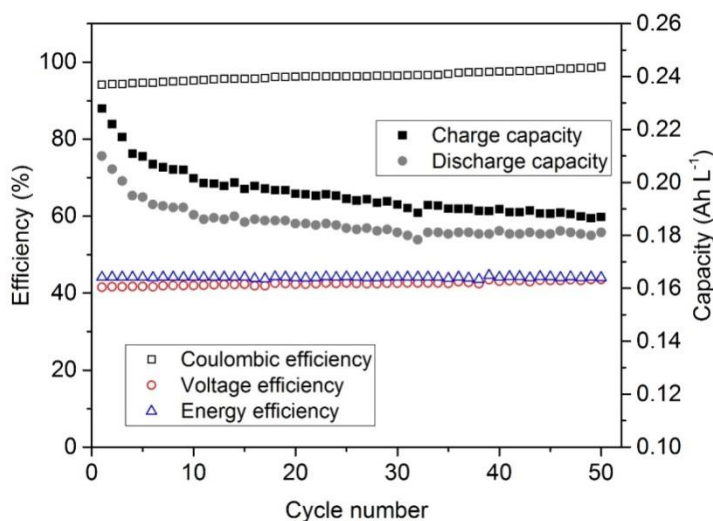


Figure 4. Cycling efficiencies and capacity of the battery with TEATFSI as the supporting electrolyte.

The efficiencies and the lifetimes of the batteries with different supporting electrolytes are listed in Table 1. The batteries with $TBABF_4$, and $TBAPF_6$ as the supporting electrolytes could not

work smoothly due to the sluggish diffusion at the electrodes. The battery with EMIMTFSI shows the lowest efficiencies. The average CE of the batteries with TEABF₄, TEAPF₆ and TEATFSI are similar, while the VE and EE of the battery containing TEATFSI are much higher than those of the other two. The battery with TEATFSI also shows the best stability. It is well known that the irreversible reactions among redox species would lead to the degradation of the flow battery system. The supporting electrolytes containing BF₄⁻, PF₆⁻ and EMIM⁺ may react with the free radicals of active substances, which reduces the efficiency and cycle life of the batteries. The stability of the battery have been improved obviously comparing with the previous work, in which seven stable cycles were obtained with BP as the anolyte and TEAPF₆ as the supporting electrolyte [13].

Table 1. Cyclic charge-discharge characteristics of the batteries with different supporting electrolytes

Supporting Electrolyte	CE (%)	VE (%)	EE (%)	Cycle numbers
TEABF ₄	93	20	28	15
TEAPF ₆	97	31	30	15
EMIMTFSI	17	2	10	5
TEATFSI	97	46	44	50

4. CONCLUSION

In this work, an all-organic RFB is fabricated with BP and DBB as anode and cathode active species, respectively. Various ionic liquids are investigated as the supporting electrolytes in AN solvent. The battery with TEATFSI as the supporting electrolyte shows an open voltage of 2.95 V. The electrode reactions are under diffusion control, and the cation of the supporting electrolyte shows a great influence on the diffusion coefficients. The anodic and cathodic diffusion coefficients in the battery containing TEATFSI are $1.21-1.43 \times 10^{-5} \text{ cm}^2 \text{ s}^{-1}$ and $0.89-1.16 \times 10^{-5} \text{ cm}^2 \text{ s}^{-1}$, respectively. During 50 charge-discharge cycles, the battery with TEATFSI as the supporting electrolyte exhibits stable CE, VE and EE of 97%, 46% and 44%, respectively, while the capacity of the battery decreases gradually. The VE, EE and stability of the battery with TEATFSI are much higher than those with other common supporting electrolytes such as TEABF₄ and TEAPF₆.

ACKNOWLEDGEMENTS

The financial support of NSF of China under contract numbers 21636007. The work has been also supported by the Program of Introducing Talents to the University Disciplines under file number B06006, and the Program for Changjiang Scholars and Innovative Research Teams in Universities under file number IRT 0641.

References

1. P. Bajpai and V. Dash, *Renewable Sustainable Energy Rev.*, 16 (2012) 2926.
2. J. Cho, S. Jeong and Y. Kim, *Prog. Energy Combust. Sci.*, 48 (2015) 84.

3. S. Hameer and J.L. van Niekerk, *Int. J. Energy Res.*, 39 (2015) 1179.
4. G. Kear, A.A. Shah and F.C. Walsh, *Int. J. Energy Res.*, 36 (2012) 1105.
5. M. Ulaganathan, V. Aravindan, Q.Y. Yan, S. Madhavi, M. Skyllas-Kazacos and T.M. Lim, *Adv. Mater. Interfaces*, 3 (2016) 1500309.
6. B.R. Chalamala, T. Soundappan, G.R. Fisher, M.R. Anstey, V.V. Viswanathan and M.L. Perry, *Proc. IEEE*, 102 (2014) 976.
7. A.Z. Weber, M.M. Mench, J.P. Meyers, P.N. Ross, J.T. Gostick and Q.H. Liu, *J. Appl. Electrochem.*, 41 (2011) 1137.
8. K. Gong, Q.R. Fang, S. Gu, S.F.Y. Li and Y.S. Yan, *Energy Environ. Sci.*, 8 (2015) 3515.
9. J.A. Kowalski, L. Su, J.D. Milshtein and F.R. Brushett, *Curr. Opin. Chem. Eng.*, 13 (2016) 45.
10. C. Buhrmester, J. Chen, L. Moshurchak, J. Jiang, R.L. Wang and J.R. Dahn, *J. Electrochem. Soc.*, 152 (2005) A2390.
11. J.H. Huang, L. Su, J.A. Kowalski, J.L. Barton, M. Ferrandon, A.K. Burrell, F.R. Brushett and L. Zhang, *J. Mater. Chem. A*, 3 (2015) 14971.
12. J. Huang, B. Pan, W. Duan, X. Wei, R.S. Assary, L. Su, F.R. Brushett, L. Cheng, C. Liao, M.S. Ferrandon, W. Wang, Z. Zhang, A.K. Burrell, L.A. Curtiss, I.A. Shkrob, J.S. Moore and L. Zhang, *Sci. Rep.*, 6 (2016) 32102.
13. X.Q. Xing, Y.J. Huo, X. Wang, Y.C. Zhao and Y.D. Li, *Int. J. Hydrogen Energy*, 42 (2017) 17488.
14. J.A. Kowalski, M.D. Casselman, A.P. Kaur, J.D. Milshtein, C.F. Elliott, S. Modekrutti, N.H. Attanayake, N.J. Zhang, S.R. Parkin, C. Risko, F.R. Brushett and S.A. Odom, *J. Mater. Chem. A*, 5 (2017) 24371.
15. M. Milton, Q. Cheng, Y. Yang, C. Nuckolls, R. Hernandez Sanchez and T.J. Sisto, *Nano Lett.*, 17 (2017) 7859.
16. A.A. Shinkle, T.J. Pomaville, A.E.S. Sleightholme, L.T. Thompson and C.W. Monroe, *J. Power Sources*, 248 (2014) 1299.
17. K. Xu, *Chem. Rev.*, 104 (2004) 4303.
18. K. Teramoto, T. Nishide, S. Okumura, K. Takao and Y. Ikeda, *Electrochemistry*, 82 (2014) 566.
19. A. Ejigu, P.A. Greatorex-Davies and D.A. Walsh, *Electrochem. Commun.*, 54 (2015) 55.
20. N. Heiland, *Int. J. Electrochem. Sci.*, (2016) 9254.
21. C.S. Sevov, D.P. Hickey, M.E. Cook, S.G. Robinson, S. Barnett, S.D. Minter, M.S. Sigman and M.S. Sanford, *J. Am. Chem. Soc.*, 139 (2017) 2924.
22. X.L. Wei, W.T. Duan, J.H. Huang, L. Zhang, B. Li, D. Reed, W. Xu, V. Sprenkle and W. Wang, *ACS Energy Lett.*, 1 (2016) 705.
23. X. Wei, W. Xu, J. Huang, L. Zhang, E. Walter, C. Lawrence, M. Vijayakumar, W.A. Henderson, T. Liu, L. Cosimbescu, B. Li, V. Sprenkle and W. Wang, *Angew. Chem., Int. Ed.*, 54 (2015) 8684.
24. K. Xu, S.P. Ding and T.R. Jow, *J. Electrochem. Soc.* 146 (1999) 4172.
25. J.D. Milshtein, J.L. Barton, R.M. Darling and F.R. Brushett, *J. Power Sources*, 327 (2016) 151.
26. W.T. Duan, R.S. Vemuri, J.D. Milshtein, S. Laramie, R.D. Dmello, J.H. Huang, L. Zhang, D.H. Hu, M. Vijayakumar, W. Wang, J. Liu, R.M. Darling, L. Thompson, K. Smith, J.S. Moore, F.R. Brushett and X.L. Wei, *J. Mater. Chem. A*, 4 (2016) 5448.
27. R.A. Potash, J.R. McKone, S. Conte and H.D. Abruña, *J. Electrochem. Soc.*, 163 (2015) A338.
28. S.K. Park, J. Shim, J. Yang, K.H. Shin, C.S. Jin, B.S. Lee, Y.S. Lee and J.D. Jeon, *Electrochem. Commun.*, 59 (2015) 68.